Article

Photoisomerization Mechanism of 11-cis-Locked Artificial Retinal Chromophores: Acceleration and Primary Photoproduct Assignment

De Vico, Marco Garavelli, Fernando Bernardi, and Massimo Olivucci

J. Am. Chem. Soc., **2005**, 127 (8), 2433-2442• DOI: 10.1021/ja045747u • Publication Date (Web): 03 February 2005

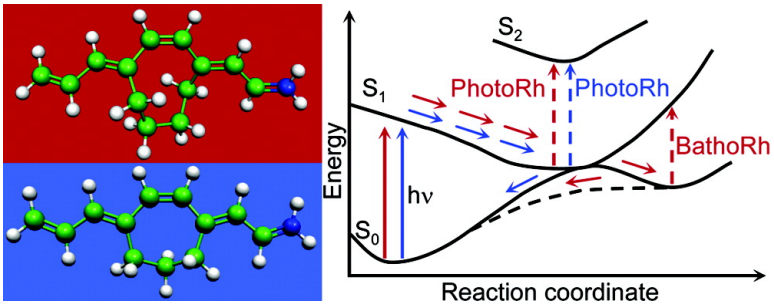

More About This Article

Additional resources and features associated with this article are available within the HTML version:

- Supporting Information
- Links to the 2 articles that cite this article, as of the time of this article download
- Access to high resolution figures
- Links to articles and content related to this article
- Copyright permission to reproduce figures and/or text from this article

View the Full Text HTML

J|A|C|S
ARTICLES
Published on Web 02/03/2005

Photoisomerization Mechanism of 11-cis-Locked Artificial Retinal Chromophores: Acceleration and Primary Photoproduct Assignment

Luca De Vico,[†] Marco Garavelli,*[,§] Fernando Bernardi,[§] and Massimo Olivucci*[,†,‡]

Contribution from the Dipartimento di Chimica, Università di Siena, via De Gasperi 2 Siena, I-53100 Italy, Centro per lo Studio dei Sistemi Complessi, Via Tommaso Pendola 37, Siena I-53100 Italy, and Dipartimento di Chimica "G. Ciamician", Università di Bologna, via Selmi 2, Bologna, I-40126 Italy

Received July 15, 2004; E-mail: olivucci@unisi.it; marco.garavelli@unibo.it.

Abstract: CASPT2//CASSCF/6-31G* photochemical reaction path computations for two 4-*cis*-nona-2,4,6,8-tetraeniminium cation derivatives, with the 4-cis double bond embedded in a seven- and eight-member ring, are carried out to model the reactivity of the corresponding ring-locked retinal chromophores. The comparison of the excited state branches of the two reaction paths with that of the native chromophore, is used to unveil the factors responsible for the remarkably short (60 fs) excited state (S_1) lifetime observed when an artificial rhodopsin containing an eight member ring-locked retinal is photoexcited. Indeed, it is shown that the strain imposed by the eight-member ring on the chromophore backbone leads to a dramatic change in the shape of the S_1 energy surface. Our models are also used to investigate the nature of the primary photoproducts observed in different artificial rhodopsins. It is seen that only the eight member ring-locked retinal model can access a shallow energy minimum on the ground state. This result implies that the primary, photorhodopsin-like, transient observed in artificial rhodopsins could correspond to a shallow excited state minimum. Similarly, the second, bathorhodopsin-like, transient species could be assigned to a ground state structure displaying a nearly all-trans conformation.

1. Introduction

The protonated Schiff base of retinal (PSB) is the chromophore of rhodopsin proteins.[1,2] These include the retina visual pigment of animals (rhodopsin), the proton and chloride pumping pigments of *Halobacterium halobium* (bacteriorhodopsin and halorhodopsin respectively) and other bacterial light sensing pigments (sensory rhodopsins). The biological activity of rhodopsins is triggered by the light-induced cis−trans isomerization of the corresponding chromophores that, in turn, induce a conformational change in the protein.[2] This photochemical step is usually referred as the primary event of the protein photocycle.

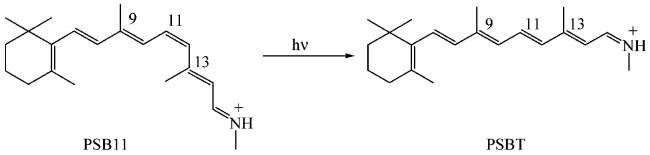

Time-resolved spectroscopic observations indicate that both the photoisomerization time scale and the excited-state lifetime (obtained through fluorescence measurements) of PSB are environment dependent. Most remarkably, in rhodopsin the excited-state lifetime of the *11-cis* PSB chromophore (PSB11) is ca. 150 fs[3] and its photoisomerization to *all-trans* PSB (PSBT) takes place in 200 fs.[4] This behavior is very different from that observed for the same chromophore in solution where, for instance, the lifetime has a dominant 3 ps component.[5] It is thus apparent that the protein is able to "catalyze" (i.e., speed up) the PSB11 → PSBT reaction with respect to the solution environment.

[†] Dipartimento di Chimica, Università di Siena.
[‡] Centro per lo Studio dei Sistemi Complessi.
[§] Dipartimento di Chimica "G. Ciamician", Università di Bologna.

(1) Shichida, Y.; Yoshizawa, T. In *CRC Handbook of Organic Photochemistry and Photobiology*; Second Edition ed.; Horspool, W., Lenci, F., Eds.; CRC Press: Boca Raton FL, 2004, p 125; Needleman, R. In *CRC Handbook of Organic Photochemistry and Photobiology*; Horspool, W. M., P.-S. Song, Ed.; CRC Press: Boca Raton, FL, 1995; Ottolenghi, M.; Sheves, M. *Isr. J. Chem.* **1995**, *35*, 193−513; Wald, G. *Science* **1968**, *162*, 230−239; Yoshizawa, T.; Kuwata, O. In *CRC Handbook of Organic Photochemistry and Photobiology*; Horspool, W. M., P.-S. Song, Ed.; CRC Press: Boca Raton, FL, 1995.
(2) Kandori, H.; Shichida, Y.; Yoshizawa, T. *Biochemistry (Moscow)* **2001**, *66*, 1197−1209; Mathies, R. A.; Lugtenburg, J. In *Handbook of Biological Physics*; Stavenga, D. G., de Grip, W. J., Pugh, E. N., Ed.; Elsevier Science B. V., 2000; Vol. 3.
(3) Kandori, H.; Sasabe, H.; Nakanishi, K.; Yoshizawa, T.; Mizukami, T.; Shichida, Y. *J. Am. Chem. Soc.* **1996**, *118*, 1002−1005.
(4) Mathies, R. A.; Cruz, C.-H. B.; Pollard, T. W.; Shank, C. V. *Science* **1988**, *240*, 777−779.
(5) Kandori, H.; Katsuta, Y.; Ito, M.; Sasabe, H. *J. Am. Chem. Soc.* **1995**, *117*, 2669−2670; Lugonov, S. L.; Song, L.; El-Sayed, M. A. *J. Phys. Chem.* **1996**, *100*, 18586−18591.

10.1021/ja045747u CCC: $30.25

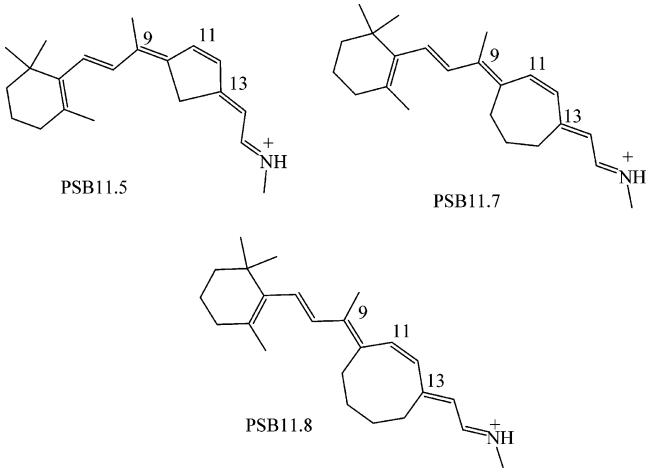

Large changes in excited-state lifetime have also been observed along a series of artificial pigments where the native PSB chromophores have been substituted with synthetic 11-cis *locked* chromophores.[3] In these molecules, the torsional deformation of the reactive double bond (e.g., the 11-cis double bond) is restrained since the double bond is part of a cyclic moiety. For this reason, the formation of a stable PSBT photoproduct is not expected and the photolysis of the artificial pigment leads to a rapid reconstitution of the starting material. On the other hand, a varied spectrum of excited-state lifetimes has been observed as a function of the ring size. For instance, an 85 ps *increase* in excited-state lifetime, along with fluorescence, is observed in an artificial rhodopsin (Rh5) where the chromophore features an 11-cis double bond embedded in a five-member ring (PSB11.5).[6] In contrast, in the different artificial rhodopsins (Rh7 and Rh8) where the 11-cis double bond is embedded in a seven (PSB11.7) and an eight (PSB11.8) member ring, respectively, one observes no fluorescence, suggesting that these chromophores are flexible enough to allow for rapid excited-state relaxation. Furthermore, Rh8 features a 90 fs *decrease*[3] in excited-state lifetime with respect to the ca. 150 fs of wild-type Rh. In other words while, as expected, the five member ring lock prevents the 11-cis → all-trans excited-state motion dominating the evolution toward the $S_1 \rightarrow S_0$ decay channel, the eight member ring lock of PSB11.8 seems to be able to accelerate this process.

Along the previous series of artificial rhodopsins, one observes a remarkable difference in the appearance of the transient photoproducts. In fact, while no photoproduct has been detected for Rh5, photolysis of Rh7 leads to a transient photoproduct with a 580 nm λ_{max}.[6] Similarly, photolysis of the less strained Rh8 system leads to the appearance of two distinct and sequential photoproducts, with a 585 and 577 nm λ_{max}, respectively.[7]

These results have been interpreted according to a reaction mechanism proposed by Mizukami et al.,[7] where the transients absorbing at 580 and 585 nm are assumed to correspond to analogues of the primary photoproduct photorhodopsin (photoRh) and the absorption at 577 nm is assumed to be associated to production of a bathorhodopsin (bathoRh) analogue. The fact that locks of different size determine the appearance of a different number of Rh photoproducts, as well as the fact that the eight member ring lock speeds up the excited-state decay, appears of great interest in the context of the investigation of the photoisomerization mechanism of PSBs. Indeed, it is apparent that the different degree of torsional flexibility associated to each ring lock must be related to the type and number of transient species generated, as well as augmented excited-state decay rate. As stressed below, the investigation of these ring strain effects, via the mapping of the intrinsic excited-state reaction path of PSB11.7 and PSB11.8, represents the main research target of the present report.

Recently, we reported the CASSCF photoisomerization paths of a series of PSB models, showing the relationship between molecular structure and the shape of the potential energy surface.[8] In the present work, we report CASPT2//CASSCF photoisomerization and relaxation path computations to achieve information about the intrinsic behavior of locked retinal chromophores after photoexcitation. Following previous results,[9] such computational strategy has been successfully used to investigate the PSB11 model 4-*cis*-γ-methylnona-2,4,6,8-tetraeniminium cation **1**.[10,11] This model has been validated by computing the absorption and fluorescence maxima, the change in dipole moment and by simulating the resonance Raman spectra of PSB11 and its ^{13}C isotopomers.[12] The computed data compare well with the corresponding experimental quantity in solution, suggesting that the terminal double bond of PSB11, which is part of the β-ionone ring, does not conjugate effectively with the remaining part of the π-system.

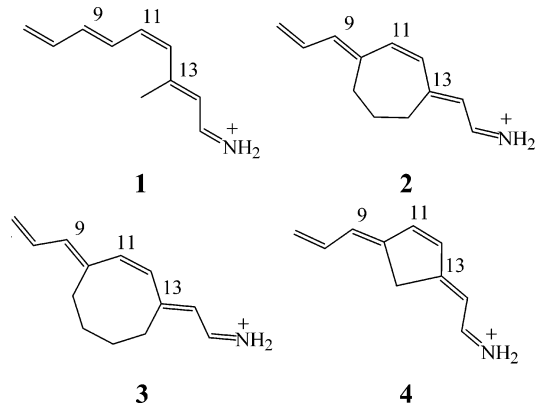

As reported in ref 11, photoisomerization path computations for **1** have demonstrated that the S_1 reaction coordinate (S_1 corresponds to the 1 B_u-like—i.e., hole-pair—spectroscopic state of polyenes) is sequentially dominated by two substantially uncoupled modes (see Figure 1a for a schematic view of the structure of the S_1 potential energy surface of **1**). The first mode is totally symmetric and drives the initially planar system out of the Franck−Condon point (**FC**) through a concerted double-bond stretch and single-bond compression. The second mode

(6) Kandori, H.; Matuoka, S.; Shichida, Y.; Yoshizawa, T.; Ito, M.; Tsukida, K.; Balogh-Nair, V.; Nakanishi, K. *Biochemistry* **1989**, *28*, 6460−6467.
(7) Mizukami, T.; Kandori, H.; Shichida, Y.; Chen, A.-H.; Derguini, F.; Caldwell, C. G.; Bigge, F.; Nakanishi, K.; Yoshizawa, T. *Proc. Natl. Acad. Sci. U.S.A.* **1993**, *90*, 4072−4076.
(8) Sinicropi, A.; Migani, A.; De Vico, L.; Olivucci, M. *Photochem. Photobiol. Sci.* **2003**, *2*, 1250−1255.
(9) Garavelli, M.; Celani, P.; Bernardi, F.; Robb, M. A.; Olivucci, M. *J. Am. Chem. Soc.* **1997**, *119*, 6891−6901.
(10) Garavelli, M.; Vreven, T.; Celani, P.; Bernardi, F.; Robb, M. A.; Olivucci, M. *J. Am. Chem. Soc.* **1998**, *120*, 1285−1288.
(11) Gonzalez-Luque, R.; Garavelli, M.; Bernardi, F.; Merchan, M.; Robb, M. A.; Olivucci, M. *Proc. Natl. Acad. Sci. U.S.A.* **2000**, *97*, 9379−9384.
(12) Garavelli, M.; Negri, F.; Olivucci, M. *J. Am. Chem. Soc.* **1999**, *121*, 1, 1023−1029.

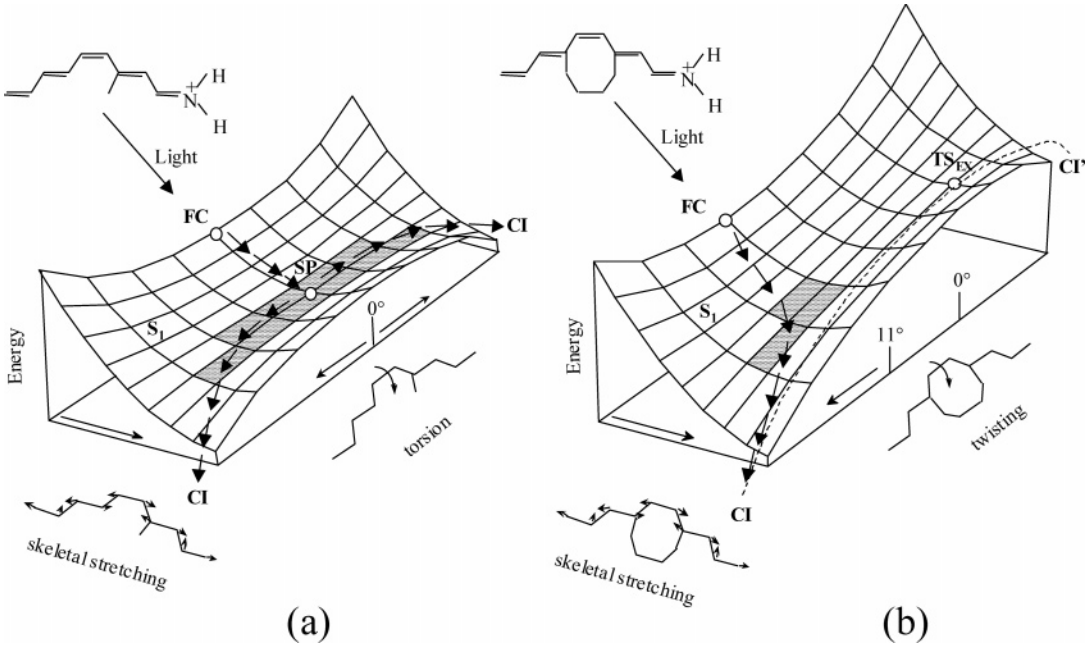

Figure 1. Schematic illustration of the two-mode structure of the S_1 energy surface along the excited-state isomerization path for (a) the PSB11 model **1** and (b) the PSB11.8 model **3** in isolated conditions. The stream of arrows on the S_1 surfaces represents the two-mode reaction coordinate starting at **FC**. The dashed line represents the path connecting the two conical intersection funnels entered via "clockwise" and "counterclockwise" torsional deformation, respectively. Point **SP** corresponds to a flat energy minimum (i.e., a metastable species) where the torsional deformation leading to two degenerate $S_1 \rightarrow S_0$ decay channels **CI** begins. Similarly, point $\mathbf{TS_{ex}}$ represents a transition structure connecting the non degenerate **CI** and **CI′** decay channels. The shaded areas corresponds to the flat S_1 energy plateau discussed in the text.

is asymmetric and is dominated by a cis−trans isomerization motion initiated after depopulation of a very flat planar energy minimum (**SP**). Evolution along this mode leads to a conical intersection funnel (**CI**) where the chromophore displays a ca. 90° twisted central double bond and where fully efficient decay to the ground state takes place.

In analogy with model **1**, in the present work we use the 4-*cis*-nona-2,4,6,8-tetraeniminium cation derivative **2** as a model of PSB11.7 and **3** as a model of PSB11.8. We will show that, while **2** features an S_1 energy surface remarkably similar to that of the unlocked model PSB11 (see Figure 1a), **3** displays an S_1 energy surface with the structure shown in Figure 1b. This surface is asymmetric with respect to the clockwise and counterclockwise torsion due to the lack of planarity of the chromophore. As a consequence, **3** will experience an initial relaxation characterized by a coupled stretching-torsional motion and not by the only stretching as in **1**. The same models will also be used to investigate the effect of the different size locks on the photoproducts appearance, assuming that this is a consequence of intrinsic chromophore factors. In other words, in PSB11.7 and PSB11.8 the ring strain (in particular the Pitzer strain[13]) would alter the structure of the S_1 force field of the native PSB11 conjugated backbone in such a way to restrain (or allow) the formation of certain intermediates and, in the case of Rh8, accelerate the evolution toward the $S_1 \rightarrow S_0$ decay channel. In the framework of this hypothesis, the results of relaxation path computations starting at the CI point of **2** and **3** call for a substantial revision of Scheme 1 and provide evidence that, indeed, the formation of a single photoproduct or of two sequential photoproducts associated to photoRh and bathoRh analogues is a function of the ring size.

(13) Eliel, E. L.; Wilen, S. H. *Stereochemistry of Organic Compounds, Cap. 9*; Wiley & Sons: New York, 1994.

Scheme 1

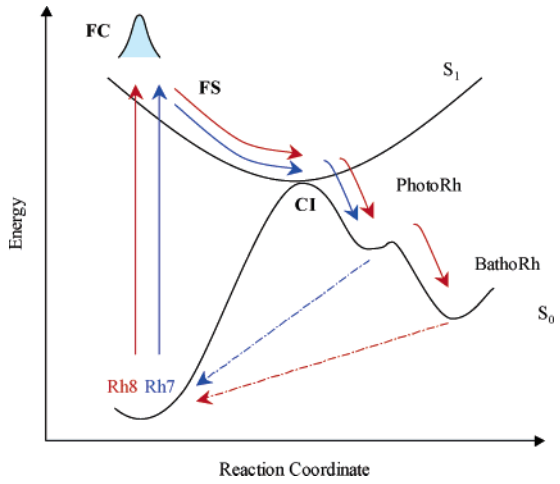

2. Computational Details

Structure optimization and relaxation path mapping have been carried out using fully unconstrained ab initio quantum chemical computations in the framework of the CASPT2//CASSCF/6-31G* strategy.[11,14] Relaxation paths were computed in terms of minimum energy path (MEP) in mass-weighted coordinates, using the IRD methodology.[15] The CASPT2//CASSCF strategy requires that the reaction coordinate is computed at the complete active space self-consistent field (CASSCF) level and that the corresponding energy profile is re-evaluated on the multiconfigurational second-order Møller−Plesset perturbation theory level (here we used the CASPT2 method[16] implemented in MOLCAS-

(14) De Vico, L.; Page, C. S.; Garavelli, M.; Bernardi, F.; Basosi, R.; Olivucci, M. *J. Am. Chem. Soc.* **2002**, *124*, 4124−4134.
(15) Bearpark, M. J.; Robb, M. A.; Schlegel, H. B. *Chem. Phys. Lett.* **1994**, *223*, 269; Celani, O.; Robb, M. A.; Garavelli, M.; Bernardi, F.; Olivucci, M. *Chem. Phys. Lett.* **1995**, *243*, 1.
(16) Andersson, K.; Malmqvist, P.-Å.; Roos, B. O. *J. Chem. Phys.* **1992**, *96*, 1218.

5)[17] to take into account the effect of electron dynamic correlation.

All computations employed the 6-31G* basis set and an active space comprising 10 electrons in 10 orbitals. This includes the full π-system. All geometry optimizations were carried out using the GAUSSIAN98 suite of programs.[18]

Energy minima and transition structures of the electronic ground state were optimized using a single root CASSCF wave function, while minima and transition structures of the electronic first excited state were optimized using a two roots (S_0, S_1) state average (0.5, 0.5) CASSCF wave function. The S_1 and S_0 potential energy surfaces were connected through Conical Intersections (CI),[19] whose optimizations were performed using the methods available in GAUSSIAN98. Recently, we demonstrated[20] that CASSCF/6−31G* optimized CIs of retinal models are, geometrically, substantially equal to those optimized using an higher level of theory (CAPST2) and larger active space.

A two roots (S_1, S_0) state average (0.5, 0.5) CASSCF wave function S_1 MEP calculation was performed to connect the Franck−Condon point of **3** to the S_1/S_0 CI; analogously, two MEP calculations were performed along the potential energy surface of **2** to connect the S_1 transition state to the minimum and to the S_1/S_0 CI. For each of the CIs, a S_0 MEP was computed using a single root wave function, connecting the chosen CI to the S_0 reagent or product minimum.

As stated before, energies of stationary points, CIs and selected points along the MEPs have been re-evaluated using single point calculations performed at the CASPT2 level of theory. For each geometry, a three roots (S_0, S_1, S_2) state-average (0.33, 0.33, 0.33) CASSCF wave function was used as reference function for evaluating the CASPT2 energies.

The CI energy of the two models were also re-evaluated at the CASPT2 level of theory using the larger basis-set 6-31G(d,p) that includes diffuse functions. Results are reported in Table 2 in the Supporting Information Section. The calculation was performed to check the consistency of the previous results when adding diffuse function. Since no sensible variation in S_0/S_1 energy difference was found, the usage of diffuse function can be considered not influent on the considered models.[21]

3. Results

3.1 Conformational Structure of the PSB11.8 Chromophore Model. While the PSB11 model **1** admits a single planar conformer,[11] the eight-member ring lock in the PSB11.8 model **3** induces an out-of-plane deformation of the originally planar 4-*cis*-nona-2,4,6,8-tetraeniminium cation moiety ultimately leading to different conformers of close energy. The **Half-chair**, **Boat-1**, and **Boat-2** structures displayed in Figure 2 were located within a 1 kcal mol^{-1} energy range.[22] It is apparent from Figure 2 that, in all conformers, the conjugated chain appears to be considerably twisted. However, while in **Half-chair** the axis of the conjugated chain is substantially linear, both the **Boat-1** and **Boat-2** structures display a considerably bent chain. As reported in Table 1 in the Supporting Information Section, **Boat-1** is 0.8 kcal mol^{-1} more stable than **Half-chair**. Despite the computed energy order, in the present paper we will only focus on the photoisomerization of **Half-chair** since this appears to be the only structure that could fit into the rhodopsin cavity.

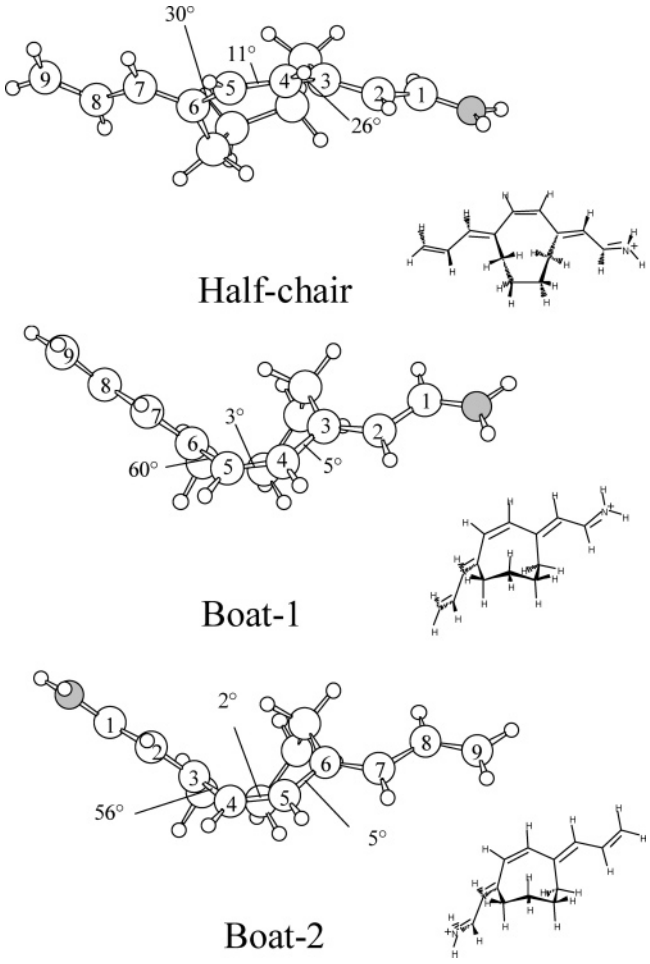

Figure 2. Ground state conformers of the PSB11.8 model **3**. The values of the three central twisting deformations correspond to the $C_7-C_6-C_5-C_4$, $C_6-C_5-C_4-C_3$, and $C_5-C_4-C_3-C_2$ dihedral angles.

The computed absorption maximum for **Half-chair** is 503 nm and therefore it is only 20 nm red-shifted with respect to the 481 nm computed for **1**.[11] This behavior seems in line with the protein absorption maxima where one has a 498 and 500 nm absorption maximum for Rh and Rh8, respectively.[23] The

(17) Andersson, K.; Barysz, M.; Bernhardsson, A.; Blomberg, M. R. A.; Cooper, D. L.; Fülscher, M. P.; Graaf, C. D.; Hess, B. A.; Karlström, G.; Lindh, R.; Malmqvist, P.-Å.; Nakajima, T.; Neogrády, P.; Olsen, J.; Roos, B. O.; Schimmelpfennig, B.; Schütz, M.; Seijo, L.; Serrano-Andrés, L.; Siegbahn, P. E. M.; Stålring, J.; Thorsteinsson, T.; Veryazov, V.; Widmark, P.-O. *MOLCAS*, Version 5.4; Lund University, Sweden: 2002

(18) Frisch, M. J.; Trucks, G. W.; Schlegel, H. B.; Scuseria, G. E.; Robb, M. A.; Cheeseman, J. R.; Zakrzewski, V. G.; Montgomery, J. A. J.; Stratmann, R. E.; Burant, J. C.; Dapprich, S.; Millam, J. M.; Daniels, A. D.; Kudin, K. N.; Strain, M. C.; Farkas, O.; Tomasi, J.; Barone, V.; Cossi, M.; Cammi, R.; Mennucci, B.; Pomelli, C.; Adamo, C.; Clifford, S.; Ochterski, J.; Petersson, G. A.; Ayala, P. Y.; Cui, Q.; Morokuma, K.; Malick, D. K.; Rabuck, A. D.; Raghavachari, K.; Foresman, J. B.; Cioslowski, J.; Ortiz, J. V.; Baboul, A. G.; Stefanov, B. B.; Liu, G.; Liashenko, A.; Piskorz, P.; Komaromi, I.; Gomperts, R.; Martin, R. L.; Fox, D. J.; Keith, T.; Al-Laham, M. A.; Peng, C. Y.; Nanayakkara, A.; Gonzalez, C.; Challacombe, M.; Gill, P. M. W.; Johnson, B.; Chen, W.; Wong, M. W.; Andres, J. L.; Gonzalez, C.; Head-Gordon, M.; Replogle, E. S.; Pople, J. A. *Gaussian 98*, Revision A.7; Gaussian, Inc.: Pittsburgh, PA, 1998

(19) Olivucci, M.; Robb, M. A.; Bernardi, F. In *Conformational Analysis of Molecules in Excited States*; Waluk, J., Ed.; Wiley-VCH: John Wiley and Sons Inc.: New York, **2000**, pp 297−366; Robb, M. A.; Garavelli, M.; Olivucci, M.; Bernardi, F. In *Reviews in Computational Chemistry*; Lipkowitz, K. B., D. B. Boyd, Ed.; Wiley-VCH: John Wiley and Sons Inc.: New York, 2000, pp 87−146.

(20) Page, C. S.; Olivucci, M. *J. Comput. Chem.* **2002**, *24*, 298−309.

(21) This effect can be explained by considering the ionic nature of the models. Indeed, a large effect given by diffuse functions can be expected when dealing with anionic species; that is because of the larger electron density of the molecule which, otherwise, could be artificially constrained on atoms. On the other hand, cation are not expected to need expansion of the basis-set, given that electron density is naturally contracted.

(22) We first performed a molecular mechanics/mm3 conformational search. The obtained structures showing all trans double bonds (with the exception of the one embedded into the ring) were optimized at the CASSCF/6-31G* level of theory. The refined geometries were then reevaluated at the CASPT2 level of theory.

(23) The fact that the absorption maximum of PSB11 and PSB11.8 are only slightly displaced from each other is also true in solution as these quantities are 445 and 435 nm respectively in methanol (when chloride is the counterion).

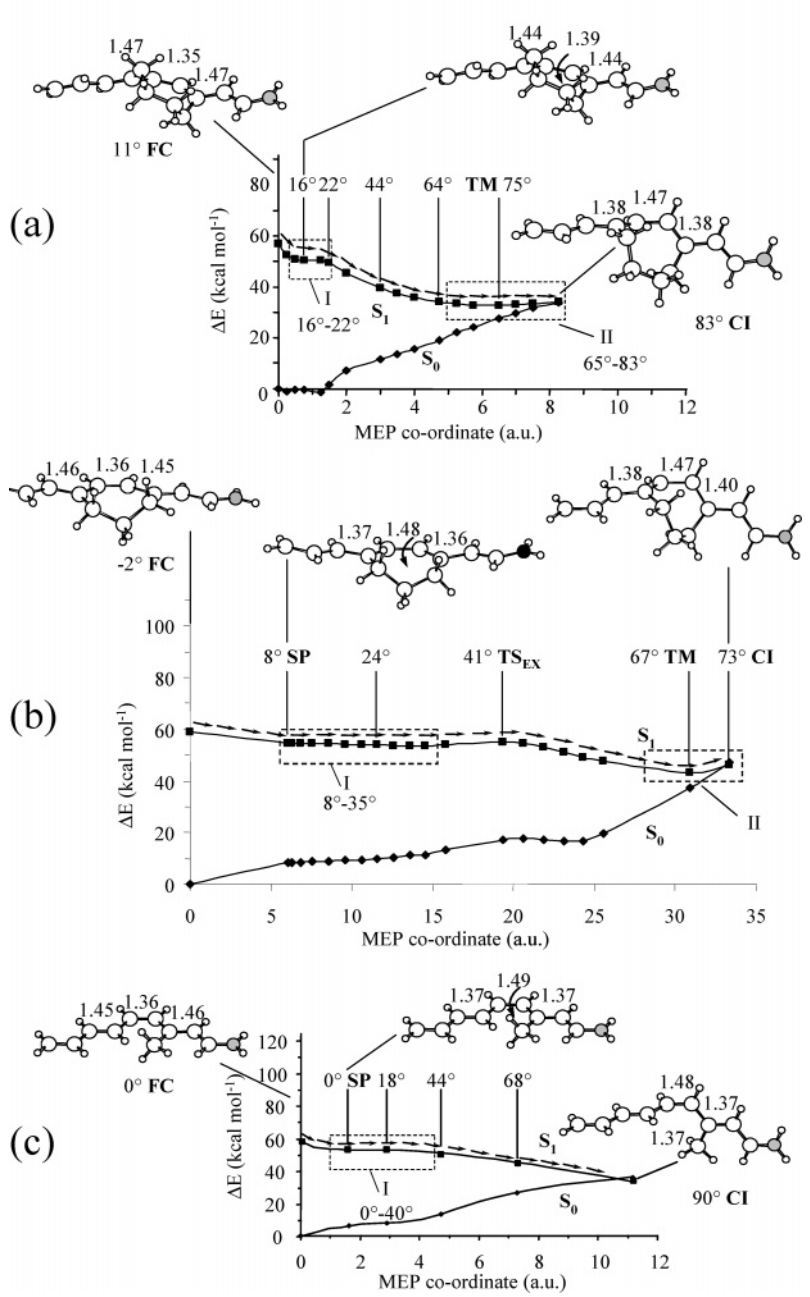

Figure 3. Energy profiles along the (a) S_1 4-cis→all-trans (11-cis → all-trans in PSB11.8) photoisomerization coordinate of **3**, (b) S_1 4-cis → all-trans (11-cis → all-trans in PSB11.7) photoisomerization coordinate of **2** and (c) S_1 4-cis→all-trans (11-cis → all-trans in PSB11) photoisomerization coordinate of **1** (data from ref 10). Full squares and full diamonds indicate the S_1 and S_0 CASPT2 energies. The structures (geometrical parameters in Å and degrees) document the progression of the molecular structure along the coordinate. **FC** is the Franck−Condon structure, **SP** corresponds to the relaxed planar species, $\mathbf{TS_{EX}}$ is a transition state, **TM** represents a relaxed twisted minimum and **CI** is the ca. 90° twisted S_1/S_0 conical intersection decay channel.

fact that the absorption maximum of **Half-chair** is slightly red-shifted with respect to **1** can be explained taking into account two basic properties of conjugated chains: (i) twisting about single bonds leads to deconjugation and therefore to a blue-shift in the absorption maximum, (ii) twisting about double bonds leads to bond breaking and therefore to a red-shift. **Half-chair** features an 11° twisted central 4-cis double bond (i.e., the one corresponding to the 11-cis double bond of PSB11.8) and the two adjacent single bonds (positions 3 and 5) twisted of 26° and 30° respectively. Thus, in this conformer, the red-shift and blue-shift effects partially cancel each other. This appears to be in line with the 481 nm blue-shifted computed absorption maximum of **Boat-1**. In fact, this conformer features a substantially planar 4-cis double bond but a 60° twisted adjacent single bond (position 5), leading to a dominant deconjugating effect. The same explanation is in line with the fact that the PSB11.5 model **4**, featuring a fully planar conjugated backbone, has a computed absorption maximum of 485 nm,[14] i.e., virtually the same as that of the unlocked chromophore **1** (481 nm). In the following the label **3** will be used to indicate exclusively the **Half-chair** conformer.

3.2 Excited-State Isomerization Path of Models 3 and 2. In Figure 3a we present the result of excited-state MEP computations for **3**. Only S_0 and S_1 CASPT2 results are reported in figure, while complete results (S_0, S_1, and S_2 CASPT2 and S_1 CASSCF) are given in Figure 6S in the Supporting

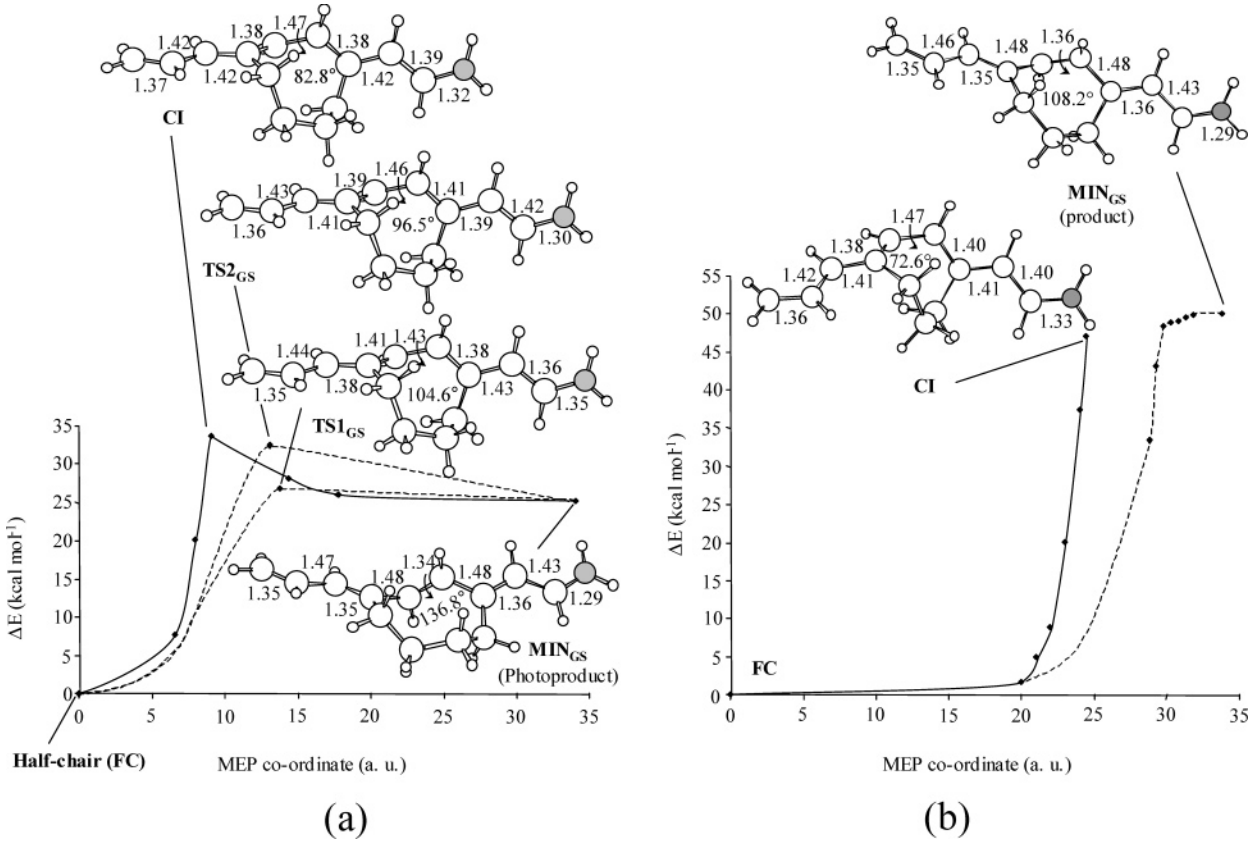

Figure 4. (a) CASPT2 energy profiles along the S_0 relaxation paths (**CI** → **MIN$_{GS}$** and **CI** → **FC**, full line) and reactant reconstitution paths (**MIN$_{GS}$** → **TS1$_{GS}$** → **FC** and **MIN$_{GS}$** → **TS2$_{GS}$** → **FC**, dashed line) for the PSB11.8 model **3**. (b) CASPT2 energy profiles along the S_0 relaxation paths (**CI** → **FC**, full line) and reactant reconstitution paths (**MIN$_{GS}$** → **FC**, dashed line) for the PSB11.7 model **2**. Structures corresponding to the energy minimums and transition states are also reported (geometrical parameters in Å and degrees). The structure of the conical intersections of Figure 3a,b are also reported to allow comparison with the other structures.

Information Section. To describe the effect of the Pitzer (i.e., torsional) strain introduced by the eight member ring lock on the shape of the 4-cis → all-trans S_1 photoisomerization path we report in Figure 3c the corresponding path for **1** taken from ref 10. As already stated above, the major difference between the two S_0 equilibrium structures (i.e., the **FC** points) is the large twisting deformation of the central portion of the conjugated chain of **3**. Despite this difference it is apparent from inspection of Figure 3, parts a and c, that the two paths display the same general structure. In particular, for both paths the S_0, S_1, and S_2 energy profiles have the same structure with the S_2 (S_2 corresponds to the singlet $2A_g$-like—i.e., dot−dot, dark excited state of polyenes) energy profile always more than 15.0 kcal mol^{-1} higher than the S_1 state (see Figure 6S in the Supporting Information Section). Thus, as previously reported,[11] our computations show that only the S_1 and S_0 potential energy surfaces are involved in photoisomerization of PSBs. For this reason, in the following we will discuss exclusively these energy surfaces.

In contrast to their general structures, the reaction coordinates and energy profiles of the excited-state isomerization path of **3** and **1** are remarkably different. A first difference is found in the **FC** region. In fact, as mentioned above (see Figure 1), the initial relaxation of the unlocked chromophore is dominated by an in-plane stretching motion leading to a planar stationary point **SP**. The following torsional relaxation starts at **SP** and develops along an extended energy plateau that ends after a ca. 40° twisting deformation (see dashed frame in Figure 3c). In contrast, **3** relaxes along a coordinate characterized by highly coupled stretching and torsional deformations. In fact, as shown in Figure 3a, the relaxation of the 11° twisted **FC** structure yields a 16° twisted structure (i.e., with a net +5° torsion increase) where, with respect to the **SP** structure of **1**, the length of the central double bond has only been slightly expanded (e.g., for the central double bond one has a 1.35 Å → 1.39 Å and 1.36 Å → 1.49 Å change for **3** and **1** respectively).

Inspection of Figure 3a reveals a second difference between the relaxation paths of **1** and **3**. In fact, while **3** displays the same energy plateau feature observed for **1** (see dashed frames I) this does not start at a planar stationary point **SP**, but at a transient 16° twisted structure. Such plateau is very short since it ends at only 22° twisting revealing a net 6° length i.e., much shorter than the 40° long energy plateau of **1**. A third difference regards the shape of the S_1 isomerization path beyond 40° torsional deformation. As shown in Figure 3c, in this region **1** leaves the energy plateau and evolves along a slope leading to a 90° twisted conical intersection **CI**. In contrast, in **3** the **CI** is located at the end of a low lying flat region of the S_1 energy surface spanned by structures featuring 65° to 83° twisting (see dashed frame II), and featuring a twisted minimum **TM** located 4 kcal mol^{-1} below the **CI**.

The excited-state MEP of model **2** shows a structure remarkably similar to that of the unlocked model **1** (compare Figure 3, parts b and c). Indeed, the nearly planar **FC** structure evolves toward an 8° twisted minimum **SP** located just 4 kcal mol^{-1} lower in energy. Similar to **1**, at **SP** the change in bond

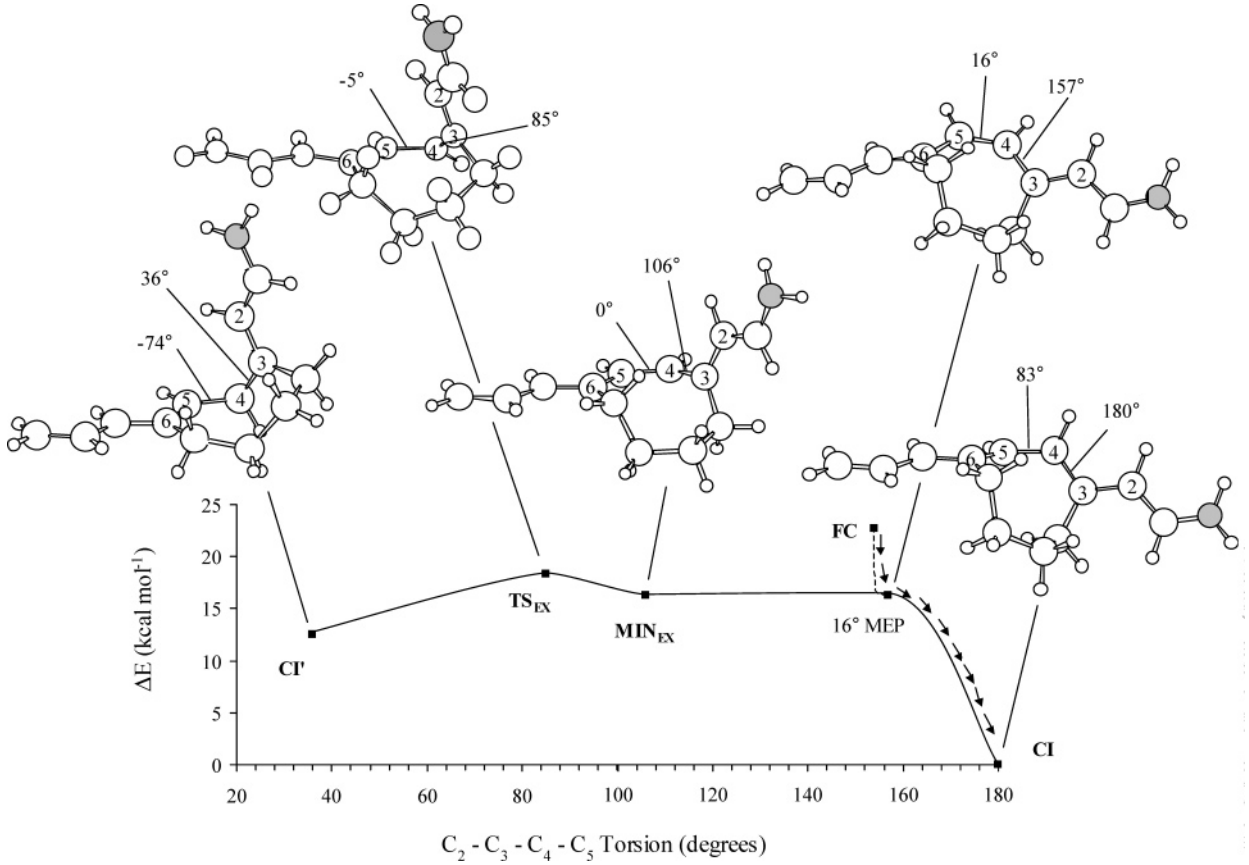

Figure 5. Structure of the S_1 potential energy surface of **3** along the **CI′ → TS$_{EX}$ → MIN$_{EX}$ → CI** path as a function of the $C_2-C_3-C_4-C_5$ torsion. The structures document the progression of the $C_3-C_4-C_5-C_6$ and $C_2-C_3-C_4-C_5$ dihedral angles along the coordinate. The stream of arrows illustrates the qualitative relationship between the excited-state reaction pathway documented in Figure 3a and the **CI → CI′** path.

order is already completed, while the torsional deformation has only increased of 10°. A nearly 30° long energy plateau (dashed frame I in Figure 3b), connects **SP** to the transition state (**TS$_{EX}$**), located 0.5 kcal mol^{-1} above **SP** and featuring a torsional deformation of 41°. After the transition state, the path evolves along a slope, reaching a twisted minimum (**TM**) which features a 67° torsional deformation and gives access to a conical intersection **CI**, located 3 kcal mol^{-1} higher in energy.

From a more quantitative point of view, the excited-state relaxation path of **2** appears to be flatter than that of **1**: for example there is a 15 kcal mol^{-1} difference in energy between **FC** and **TM** against the 25 kcal mol^{-1} energy difference between **FC** and **CI** of **1**.

3.3 Ground-State Relaxation and Reactant Reconstitution of Models 3 and 2. At **CI** the excited state species undergoes a fully efficient decay to S_0 prompting ground-state relaxation and, ultimately, photoproduct formation. To provide mechanistic information on the decay process we have computed the relaxation paths departing from **CI**.

In Figure 4a, we report two relaxation paths of **3** leading to (i) the reactant and (ii) a high energy minimum **MIN$_{GS}$** displaying an *all-trans*-nona-2,4,6,8-tetraeniminium cation moiety. Because of the high torsional strain imposed by the ring, **MIN$_{GS}$** is located ca. 25 kcal mol^{-1} higher in energy than the reactant and displays a 137° twisted "trans" central double bond. Thus, route i constitutes a photochemical reactant back-formation path while route ii leads to production of a relatively unstable all-trans photoproduct. To provide a quantitative estimate of the degree of stability of **MIN$_{GS}$** we have located two different transition structures **TS1$_{GS}$** and **TS2$_{GS}$**, both associated with the all-trans→4-cis thermal isomerization of the primary photoproduct (i.e., to thermal reactant reconstitution).[24] The magnitude of the associated reaction barriers is 1.6 and 7.2 kcal mol^{-1} respectively, indicating that **TS1$_{GS}$** defines the most efficient thermal isomerization route for the return of **MIN$_{GS}$** to the original **Half-chair** structure of **3**.

In Figure 4b is reported the reactant back-formation determined for **2**. This is the only relaxation path for this model. In fact, a minimum **MIN$_{GS}$** displaying a 108° twisted "trans" central double bond was located 3 kcal mol^{-1} above **CI**.

In the region of the CI, the S_1 energy surfaces of model **2** and **3** appear to be similar (both showing a **TM** and a higher in energy **CI**). However, the S_0 ones are quite different, giving rise to different conical intersections. Indeed, **2** shows a conical intersection with a more "sloped"[25] topography than that of **3**. As a consequence, the relatively unstable photoproduct **MIN$_{GS}$** of **3** can be reached via the photoisomerization path through the **CI**, while **MIN$_{GS}$** of **2** could be reached only via a thermal one as the **CI** gives access only to the reagent's valley. For a three-dimensional representation of the two CIs see also Scheme 5S in the Supporting Information Section.

(24) It is quite common that transition state's saddles controlling thermal cis−trans isomerization are split in two by a conical intersection peak. (see De Vico et al. *J. Am. Chem. Soc.* **2002** and Zilberg, S.; Haas, Y. *Photochem. Photobiol. Sci.* **2003**, *2*, 1256−1263) This, ultimately, leads to the appearance of two different transition states, as depicted in Scheme 5S in the Supporting Information Section.

(25) Atchity, G. J.; Xantheas, S. S.; Ruedenberg, K. *J. Chem. Phys.* **1991**, *95*, 1862−1876.

Scheme 2

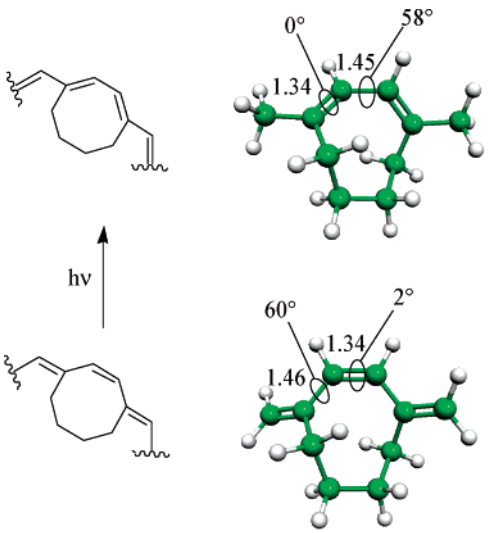

Scheme 3

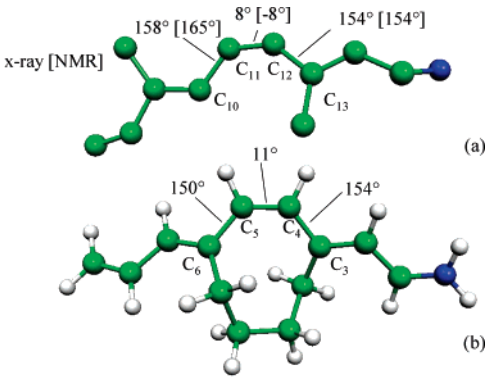

Scheme 4

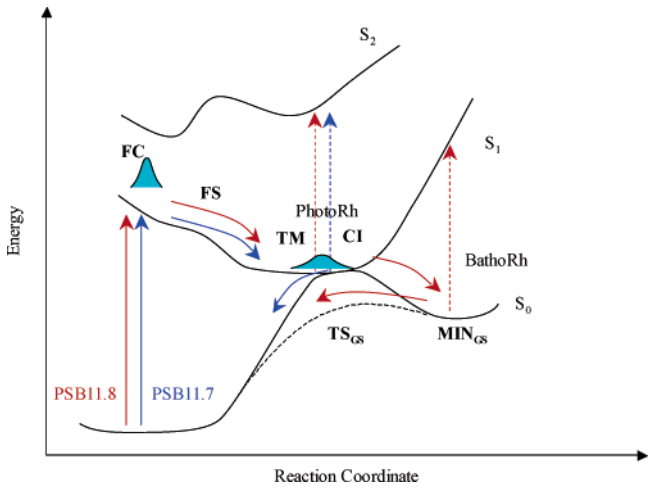

4. Discussion

4.1 Structure of the Excited-State Isomerization Path of Model 3. In this section, we discuss the effect of the eight member ring strain on the structure of the S_1 potential energy surface along the $C_3-C_4-C_5-C_6$ torsion. In the Introduction Section, we mentioned that **3** features an asymmetric excited-state potential energy surface (see Figure 1b). Indeed, transition state optimization on S_1 leads to a stationary point with a −5° twisted 4-cis double bond (**TS_{EX}**), that plays the role of the asymmetric structure SP. As shown in Figure 5, this structure connects two S_1/S_0 conical intersections, **CI′** and **CI**. **CI′** is located ca. 6 kcal mol^{-1} below **TS_{EX}** and features a −74° twisted double bond. Torsional deformation in the opposite direction displaces **TS_{EX}** toward an extended energy plateau beginning at the energy minimum **MIN_{EX}** located 2 kcal mol^{-1} below **TS_{EX}** and featuring a 0° twisted 4-cis double bond. Inspection of the **CI′**, **TS_{EX}** and **MIN_{EX}** structures reveals that the deformation along the $C_3-C_4-C_5-C_6$ torsion (i.e., the original central double bond) is not the only variable involved in the **CI′→TS_{EX}→MIN_{EX}** structural change. In fact, the molecule also undergoes a 70° torsional change about the single bond in position 3 (i.e., along the $C_2-C_3-C_4-C_5$ torsion). Evolution beyond **MIN_{EX}** leads toward the energy plateau described in Section 3.2 (this starts at the 16° twisted structure of Figure 3a. The associated MEP, starting at **FC**, is indicated by a stream of arrows), and ultimately toward the conical intersection **CI** (Figure 5).

4.2 Excited-State Lifetime Tuning: the "Spring" Effect. As mentioned in the Introduction Section, we have recently provided computational evidence that excited-state lifetime is associated with the time scale required for S_1 vibrational energy redistribution (from totally symmetric stretching modes to the weakly coupled asymmetric torsional ones) and evolution along the barrierless energy plateau located along the 11-cis→all-trans reaction coordinate.[8,11] As we shall now discuss, this mechanism provides the basis for the comprehension of the effect of the ring locks on the excited-state lifetime of the PSB11 chromophore. A *decrease* of the excited-state lifetime (i.e., a faster $S_0 \rightarrow S_1$ decay) should occur when:

(i) the coupling between the stretching and torsional coordinates is increased so that to increase the rate of vibrational energy redistribution from the initially populated **FC→SP** mode to the **SP→CI** isomerization mode and

(ii) the length of the energy plateau located along the **SP→CI** torsional mode is reduced so that the S_1 chromophore is more rapidly accelerated toward the decay channel.

The artificial PSB11.5 retinal chromophore provides one extreme case where the lock induces a dramatic *decrease* of the excited-state decay rate. In a recent work[14] we have used the PSB11.5 model **4** to investigate the origin of this effect. We found that, due to the planarity of the five member ring lock, this structure maintains a planar ground state and thus does not feature an increased coupling between stretching and torsional modes.

In contrast to PSB11.5, the PSB11.8 chromophore investigated in the present paper provides a case of dramatic *increase* of the excited-state decay rate in rhodopsin. The analysis of the computed photoisomerization path (Figure 3a) and S_1 stationary points (Figure 5) of **3** indicates that the PSB11.8 S_1 energy surface satisfies both the properties i and ii. In particular, the out-of-plane distortion of the conjugated chain induced by the lock dramatically enhances the coupling between stretching and torsional modes along the initial part of the reaction path.

In mechanistic terms, the computed data indicate that the eight member ring "lock" operates such as a spring triggered by light absorption. In fact, as described above, our computations show that, upon absorption of a photon of light, the double bond pattern of the central part of the PSB chain of **3** is changed in such a way that the positions of single and double bonds are

exchanged thus imposing a large torsional strain about the C_3-C_4, C_4-C_5, and C_5-C_6 bonds.[26] The cyclooctadiene in Scheme 2 has a ca. 60° equilibrium angle about the C_4-C_5 bond (i.e., the initial 4-cis double bond). Since the diene is a model for the excited state of **3**, 60° is the equilibrium value "imposed" by the eight member ring "spring" to the torsional deformation of the reactive bond. In other words, while the presence of the eight member ring prompts a very rapid torsional deformation away from the fluorescent state it would also partially restrain complete deformation toward the 90° **CI** decay channel. This appears to be in line with the computed energy profile of Figure 3a and with the discussion reported in Section 3.2. In other words, in contrast to **1**, structure **3** has a flat low lying segment of the S_1 path spanned by structures featuring 65° to 83° torsional deformations (frame II in Figure 3a). One could even detect a flat energy minimum at ca. 75° torsional deformation. We assigned this behavior to the effect of the cyclooctadiene-like structure of the excited-state lock.

To confirm the above assignment, we performed the same analysis, comparing the computed ground-state equilibrium conformation of a cycloheptatriene with a cycloheptadiene, as models of the S_0 and S_1 structure of the seven member ring moiety of **2** (and, in turn, PSB11.7), respectively. Both structures show a planar central bond (see Scheme 6S in Supporting Information Section), so no speed-up is expected from the seven member ring moiety. Consistently, the computed MEP indicates a slower **FC** → **CI** motion, with respect to **3**. In fact, while there is a coupling between the stretching and torsional modes in the motion out of **FC**, the presence of the long plateau and, most of all, of a transition structure (**TS_{EX}**) along the path are not consistent with an acceleration of the photoisomerization process.

As mentioned in the Introduction, we assumed, as a working hypothesis, that the fluorescence lifetime decrease observed in Rh8[3] is the consequence of an intrinsically faster decay of the locked chromophore with respect to PSB11. The results reported so far provide evidence that this is indeed the case, as the S_1 force field of the isolated PSB11.8 chromophore must effectively accelerate the chromophore toward the $S_1 \rightarrow S_0$ decay channel. Thus, in Rh8 both the protein environment and the "environment" provided by the eight member ring lock accelerate the decay of PSB11 with respect to the solution environment. This leads to the idea that the protein cavity could modify the S_1 energy surface structure of PSB11 in a way similar to the eight member ring. For instance, in Scheme 3 we compare the observed out-of-plane deformation of PSB11 in Rh (data obtained from X-ray diffraction[27] and NMR[28]) with the ground-state equilibrium structure of our PSB11.8 model **3**. It is evident that, while there are important quantitative differences between the two structures, the directions of torsional deformation are the same (in particular the deformations about the $C_{11}-C_{12}$ (8° counterclockwise) and C_5-C_4 (11° counterclockwise). In other words, one can think that the asymmetric protein cavity imposes a torsional strain on the chromophore backbone that reinforces that imposed by the eight member ring lock.

4.3 Correlation between Computed and Experimental Results: Hypothesis on the Primary Photoproduct Appearance. In this Section, we discuss the reaction mechanism for the photoisomerization of PSB11.7 and PSB11.8 on the basis of the computational results reported above.

As shown in Scheme 4, the results of the computational investigation of our PSB11.7 and PSB11.8 models agree with the initial part of the mechanistic picture of Scheme 1. An initial combined stretching/torsional relaxation from **FC** leads, within a single oscillation, to a fluorescence state (**FS**) that we assign to the first energy plateau seen in Figure 3 (dashed frames I). After that, the system reach a low-lying and flat non fluorescent (i.e., the S_1-S_0 energy gap is <20 kcal mol^{-1}) region where it could reach the conical intersection funnel. Following the decay on the ground state, the chromophore could evolve toward a ground-state intermediate featuring a ca. 140° torsion about the reconstituted "trans" double bond.[29] This intermediate can be thermally reverted to the starting material by overcoming a small energy barrier.

From Section 3.3, we know that **3** is capable to access a 137° twisted "trans" intermediate via the photochemical path, while **2** cannot do it. Furthermore, we know that, experimentally, Rh7 and Rh8 show a primary photoproduct analogue to photorhodopsin, while only Rh8 shows also the bathorhodopsin analogue photoproduct. Comparing the computed minimum energy paths of **3** and **2** in Figure 3, one should observe that the two potential energy surfaces show a region, centered on the **TM** structures, where the wave packet could spread (see dashed frames II in Figure 3). We make the assumption that this flat region of **2** and **3** could be associated with the photorodopsin primary photoproduct analogue. Of course, **2** does not show any evidence of a bathorhodopsin photoproduct analogue because the molecule immediately reverts to the initial form after decay at **CI**.

In other words, PSB11.7 and PSB11.8 reach the end of the S_1 slope before vibrational cooling. Then they cool vibrating in the **TM**−**CI** flat region (which means also back and forth between the S_1 and S_0 potential energy surfaces); we associate this condition with the photorhodopsin primary photoproduct. Finally, the chromophores relax on the ground state, triggering reactant back formation (PSB11.7) or bathorhodopsin analogue production (PSB11.8).

5. Conclusions

Above we have provided computational evidence in favor of an efficient "catalysis" of the departure of a PSB11 chromophore from its fluorescent state **FS**. An eight-member ring lock acts like a light-triggered spring that imposes a considerable Pitzer strain on the central part (i.e., $C_3-C_4-C_5-C_6$ and $C_{10}-C_{11}-C_{12}-C_{13}$ moieties in **3** and PSB11.8, respectively) of the conjugated chain of the chromophore. As discussed in Section 4.2, the strain mainly originate by the change in bond order occurring during vertical excitation (see Scheme

(26) The origin of this effect can be explained as followed (see Scheme 2). Upon photoexcitation the eight member ring moiety changes its electronic (i.e., bonding) structure passing from that of a cyclooct*ene* to that of a cyclooctadiene moiety. This change prompts a rapid adaptation of the initially planar configuration of the 4-cis double bond towards that of the skewed single bond of a cyclooctadiene moiety. This is demonstrated in Scheme 2 where we display the computed ground-state equilibrium conformation of a triene (with a cyclooctene moiety) and a diene as models of the S_0 and S_1 structure of the eight member ring moiety of **3** (and, in turn, PSB11.8), respectively.

(27) Teller, D. C.; Okada, T.; Behnke, C.; Palczewski, K.; Stenkamp, R. E. *Biochemistry* **2001**, *40*, 7761−7772.

(28) Verdegem, P. J. E.; Bovee-Geurts, P. H. M.; De Grip, W. J.; Lugtenburg, J.; De Groot, H. J. M. *Biochemistry* **1999**, *38*, 11316−11324.

(29) Despite extensive search, a S_0 trans conformer of **3** featuring a fully planarized C_4-C_5 double bond could not be located.

2) that pushes the torsional deformation of the reactive (4-cis) double bond. As a result, the 40° long energy plateau documented in the native PSB11 model **1** is reduced to a short 6° long segment suggesting a strongly decreased fluorescence lifetime.

On the basis of detailed comparison of the potential energy surface shape of **2** with that of **3** (along with the experimental data), we have presented an hypothesis onto the nature of the primary photoproduct of Rh7 and Rh8. Such hypothesis implies that the photorhodopsin-like first intermediate of these chromophores could correspond to the flat region surrounding the twisted minimum at the end of the excited state slope, where the chromophore may oscillate many times before decaying at the conical intersection funnel. Finally, the Rh8 bathorhodopsin-like photoproduct could be assigned to a ground state structure displaying a nearly trans conformation of the central double bond.

Our PSB11.8 model does not comprise the β-ionone ring. However, as previously documented for the PSB11 model **1** and discussed in the Introduction section, this approximation can be accepted if one is interested in a mechanistic description of the initial excited-state dynamics of the chromophore (say from **FC** to **FS**) where the double bond residing in the β-ionone ring does not effectively conjugate with the rest of the PSB chain. Partial or total planarization of the β-ionone moiety may occur later along the reaction, due to the bond order inversion occurring in the excited state. This bond order change together with the effect of the protein cavity must be taken into account when trying to model more rigorously the behavior of Rh7 and Rh8 beyond the bottom of the S_1 surface.

Acknowledgment. We are grateful to Prof. Kandori for helpful discussions. Funds have been provided by the Università di Siena (Progetto di Ateneo A.A. 02/04), HFSP (RG 0229/2000-M), FIRB (RBAU01EPMR), and the Università di Bologna (Funds for selected Research Topics). We wish to thank the "CINECA" for granted calculation time on their computers.

Supporting Information Available: 31 pages containing Figure 6S, Scheme 5S, Scheme 6S, CASSCF/6-31G* absolute, CASPT2/6-31G* absolute and relative energies along with wave function reference weights (Table 1) and Cartesian coordinates (Table 3) of all structures discussed in the text. Table 2 reports the 6−31G(d,p) re-evaluated CASPT2 energies of the **CI**s of model **2** and **3**. This material is available free of charge via the Internet at http://pubs.acs.org.

JA045747U